PHILOSOPHICAL TRANSACTIONS B

rstb.royalsocietypublishing.org

Research

Cite this article: Sunuwar L, Medini M, Cohen L, Sekler I, Hershfinkel M. 2016 The zinc sensing receptor, ZnR/GPR39, triggers metabotropic calcium signalling in colonocytes and regulates occludin recovery in experimental colitis. *Phil. Trans. R. Soc. B* **371**: 20150420.
http://dx.doi.org/10.1098/rstb.2015.0420

Accepted: 3 May 2016

One contribution of 15 to a Theo Murphy meeting issue 'Evolution brings Ca^{2+} and ATP together to control life and death'.

Subject Areas:
physiology, cellular biology

Keywords:
zinc, ZnR/GPR39, Ca^{2+} signalling, tight junction, intestinal epithelium, colitis

Authors for correspondence:
Israel Sekler
e-mail: sekler@bgu.ac.il
Michal Hershfinkel
e-mail: hmichal@bgu.ac.il

†These authors contributed equally to this study.

THE ROYAL SOCIETY PUBLISHING

The zinc sensing receptor, ZnR/GPR39, triggers metabotropic calcium signalling in colonocytes and regulates occludin recovery in experimental colitis

Laxmi Sunuwar†, Michal Medini†, Limor Cohen, Israel Sekler and Michal Hershfinkel

Department of Physiology and Cell Biology, Faculty of Health Sciences, Ben-Gurion University of the Negev, Beer-Sheva 84105, Israel

IS, 0000-0002-7550-1550; MH, 0000-0003-1652-1989

Impaired epithelial barrier function is a hallmark of inflammatory bowel diseases, such as colitis, contributing to diarrhoea and perpetuating inflammation. We show that the zinc sensing receptor, ZnR/GPR39, triggers intracellular Ca^{2+} signalling in colonocytes thereby inducing occludin expression. Moreover, ZnR/GPR39 is essential for epithelial barrier recovery in the dextran sodium sulfate (DSS) ulcerative colitis model. Loss of ZnR/GPR39 results in increased susceptibility to DSS-induced inflammation, owing to low expression of the tight junction protein occludin and impaired epithelial barrier. Recovery of wild-type (WT) mice from the DSS insult was faster than that of ZnR/GPR39 knockout (KO) mice. Enhanced recovery of the epithelial layer and increased crypt regeneration were observed in WT mice compared with ZnR/GPR39 KO, suggesting that ZnR/GPR39 is promoting epithelial barrier integrity following DSS insult. Indeed, cell proliferation and apical expression of occludin, following the DSS-induced epithelial erosion, were increased in WT tissue but not in ZnR/GPR39 KO tissue. Importantly, survival following DSS treatment was higher in WT mice compared with ZnR/GPR39 KO mice. Our results support a direct role for ZnR/GPR39 in promoting epithelial renewal and barrier function following DSS treatment, thereby affecting the severity of the disease. We suggest ZnR/GPR39 as a novel therapeutic target that can improve epithelial barrier function in colitis.

This article is part of the themed issue 'Evolution brings Ca^{2+} and ATP together to control life and death'.

1. Background

Inflammatory bowel diseases (IBD), including ulcerative colitis (UC) and Crohn's disease (CD), are characterized by chronic dysregulation of the mucosal layer of the gastrointestinal system [1]. They share a relapsing and remitting chronic condition and involve poorly characterized genetic component, immune dysregulation and environmental factors. Ulcerative colitis is associated with increased infiltration of inflammatory cells and oedema, distortion of crypt structure and loss of the epithelial barrier that is followed by erosion and ulcerations. Of major importance in the etiology of the disease are alterations in tight junctions [2]. Tight junctions connect the epithelial cells, and induce a continuous boundary between the lumen and the mucosal layer thereby protecting from paracellular permeation and subsequent inflammation. Occludin is a critical component of the tight junction complexes but its localization to the apical cell surface may be disrupted by pathological stimuli [3,4]. Although mechanisms underlying IBD are not fully understood, breakdown of the physical epithelial tight junction barrier often precedes the onset of inflammation. Furthermore, animal models

of experimental colitis, suggest that dysregulation of the tight junctions enhances epithelial apoptosis and induces colitis [5].

Zinc enhances functional integrity of the digestive system [6–8]. Zinc deficiency is frequently found in IBD patients and linked to attenuated renewal of the epithelium and the onset severe diarrhoea [9–11]. Consistently, zinc supplementation to Crohn's disease patients during clinical remission or in animal models of experimental colitis reduced intestinal permeability and mucosal damage [12–15]. A specific Zn^{2+} sensing receptor (ZnR) was functionally described in this tissue [16,17] and was later associated with GPR39 as the molecular moiety mediating its activity [18,19]. The ZnR/GPR39 triggers cellular Ca^{2+} signalling pathways and enhances cell proliferation, differentiation and survival [20]. The ZnR/GPR39 is prominently expressed in the gastrointestinal tract [21], and the analysis of ZnR/GPR39 knockout (KO) mice suggested a mild gastric phenotype of accelerated gastric emptying and higher volume of gastric fluid secretion [22]. Importantly, these mice have normal life expectancy. The role for ZnR/GPR39 in intestinal diseases linked to barrier function, however, had remained elusive. We show, here, that ZnR/GPR39 activates intracellular Ca^{2+} signalling and promotes occludin expression and recovery in the dextran sodium sulfate (DSS) ulcerative colitis model.

2. Material and methods

(a) Caco-2 imaging

Caco-2 colonocytic cells were grown in DMEM medium [20] containing 100 U ml^{-1} penicillin, 0.1 mg ml^{-1} streptomycin, 2 mM glutamine, 10% foetal calf serum (Biological Industries, Kibbutz Beit Haemek, Israel), 1% (v/v) nonessential amino acids (Biological Industries) and 2 mM sodium pyruvate (Sigma-Aldrich, Rehovot, Israel) in a 5% CO_2 humidified atmosphere at 37°C. Fluorescent imaging measurements were acquired on cells loaded with Fura-2 acetoxymethyl ester (AM; TEF-Labs, Austin, TX, USA) in Ringer's solution (30 min 2.5 µM). Fura-2 was excited at 340 and 380 nm, and imaged with a 510 nm long-pass filter, the ratio of the signal is shown in the traces. Bar graphs show the rate of the initial response and are the means of at least three independent experiments, with averaged responses of 7–10 cells from each of the *n* slides, as marked.

(b) Occludin recovery in Caco-2 cells

Caco-2 cells were differentiated on coverslips for 14 days. Subsequently, cells were treated with 0.05% Ca^{2+} for 16 h to deplete occludin [23] and then activation of ZnR/GPR39 was triggered by Zn^{2+} (200 µM, 2 min) in the presence or the absence of Ca^{2+} chelators. Cells were harvested into lysis buffer (50 mM HEPES, pH 7.5, 150 mM NaCl, 1 mM EDTA, 1 mM EGTA, 10% glycerol, 1% Triton X-100, 10 µM MgCl2, 25 mM NaF), in the presence of Protease Inhibitor Cocktail (1 : 50, Sigma-Aldrich). Protein concentrations were determined and whole-cell lysates (12 µg) were separated on 10% SDS-PAGE and blotted onto nitrocellulose membranes [20]. Antibodies raised against occludin (Invitrogen, Life Technologies) were used, and blots were quantified using ImageJ Gels Plugin.

(c) Induction of colitis and clinical evaluation

Experimental procedures were performed in accordance with a protocol approved by the committee for the Ethical Care and Use of Animal in Experiments at the Faculty of Health Science at Ben-Gurion University of the Negev. ZnR/GPR39 KO mice and wild-type (WT) littermates, of C57BL background, 8–10 weeks old were used in this study [22]. Mice were given DSS (MP Biomedicals) freshly prepared daily, at a concentration of 2.5% in drinking water for 6 days (disease phase), followed by 4 days of water (without DSS, recovery phase) administration. The control group received water without DSS during the whole experiment. The experimental protocol used in the current project was calibrated for this strain of mice [24]. Since high mortality rates in both genotypes were monitored using the standard protocol [25], we used 2.5% DSS for 6 days only. Mice exhibited severe disease activity clinically and histologically, after 6 days of DSS: extensive area of complete destruction of the mucosa with ulcers and active inflammation, along with small regions of architectural distortion of crypt, parallel to severe disease activity in UC patients [26].

Clinical evaluation was done daily for each mouse, by a person blind to the genotype—the disease activity index was determined by scoring changes in weight, haemoccult positivity or gross bleeding and stool consistency [25]. The score for each parameter was between 0 and 4; when 4 represents the most severe condition (table 1). The score for weight changes were obtained as percentage of initial weight. Stool blood kit (Cenogenics) was used in order to determine severity of bleeding.

Table 1. Disease activity index, adapted from [25].

score	weight loss (%)	stool consistency	occult/gross bleeding
0	none	normal	normal
1	1–5		
2	6–10	loose stools	haemoccult +
3	11–20		
4	>20	diarrhoea	gross bleeding

(d) Genotyping of mice

Polymerase chain reaction (PCR) was used to screen the mice, using tail biopsy samples that were incubated overnight at 55° in lysis buffer containing: 50 Mm KCl, 10 Mm Tris–HCl PH-8.3, 25 Mm $MgCl_2$, 0.45% NP-40, 0.45% Tween-20 and fresh proteinase K (Sigma-Aldrich). PCR was done with Red Mix (LAROVA GmbH) solution according to the manufacturer's protocol using the following primers: 5′-ACCCTCATCTTGGTGTACCT-‘3 and 5′-ATGTAGCGCTCAAAGCTGAG-‘3 (Sigma-Aldrich) that amplified a 311 bp band from the WT allele. ZnR/GPR39 KO primers were 5′-GGAACTCTCACTCGACCTGGG-‘3 and 5′-GCAGCGCA TCGCCTTCTATC-‘3 (Sigma-Aldrich) amplified a 262 bp band. After amplification, samples were mixed with Syber Green (Life Technologies) and loaded in electrophoresis agarose gel.

(e) Histological analysis

Mice were sacrificed at 0, 3, 6, 8, 10 days following the addition of DSS and distal colons were dissected. Tissues were washed in phosphate-buffered saline (PBS) solution and immediately moved to 4% paraformaldehyde (Sigma-Aldrich) for 24 h of fixation. Next, tissues were washed in ethanol at increasing concentrations (70–100%), and then moved to xylene (Biolab) and finally paraffinized. Paraffin blocks containing longitudinally positioned full-length colons were then cut into 4 µm slices and stained with haematoxylin and eosin (HE), using a standard protocol. The HE-stained tissue sections were analysed [27] by a person blind to the genotype and treatment stage. Tissues were graded by the following features: level of inflammation, severity of the oedema, extent of inflamed tissue within the wall (table 2). To directly determine the damage to the epithelial layer, we also determined level of

Table 2. Quantitative histological grading of colitis; adapted from [27].

feature graded	grade	description
inflammation	0	none
	1	slight
	2	moderate
	3	severe
severity of oedema	0	none
	1	mucosa
	2	mucosa and submucosa
	3	transmural
extent of inflamed tissue within the wall (extent of damage)	0	none
	1	mucosa
	2	mucosa and submucosa
	3	transmural
crypt damage	0	none
	1	basal 1/3 damage
	2	basal 2/3 damage
	3	only surface epithelium intact
	4	entire crypt and epithelium lost
epithelial damage (used only for the recovery phase)	0	complete regeneration or normal surface epithelium
	1	almost complete regeneration of surface epithelium
	2	regeneration of surface epithelium with crypt depletion
	3	surface epithelium not intact
	4	no epithelial repair

crypt damage within the epithelium and the general epithelial damage was determined, during the recovery phase only, as the extent of injured non-regenerated tissue along the surface. Each of the indices was blindly determined and given a grade as described in table 2. For each feature, we also scored per cent of involvement along the distal colon: 1: 1–25%, 2: 26–50%, 3: 51–75%, 4: 76–100% of total colon length. We then multiplied the grades of each of the features by the involvement score, to receive a histological index in each of the features (ranging from 0–16), the histological indices (exact values) achieved using this analysis are included in the text. For simplicity of presentation in the bar graphs, all features were normalized to the relevant score of the WT.

For occludin staining, slices were prepared as described above and were permeabilized by incubating the slices with proteinase at concentration 1 mg ml^{-1} in 37°C for 10 min (for occludin staining). Blocking was then done using normal goat serum for 30 min in room temperature. Tissues were incubated for 1 h with anti-mouse polyclonal antibodies against occludin (1 : 50) (Invitrogen) and then 1 h with a secondary anti-rabbit IgG (1 : 150) fluorescently labelled with Cy3 (Jackson ImmunoResearch). At least three images were taken from each slide using florescence microscopy at 20× magnification and a single determined set of parameters for the image acquisition. Quantitative analysis was performed by counting pixels that were stained above a predetermined threshold in a constant sized region along the mucosa in each image.

(f) Cell proliferation assay

Mice were intraperitoneally injected with 50 mg kg^{-1} of the thymidine analogue, 5-bromo-2-deoxyuridine (BrdU) 2 h before sacrifice. Paraffin sections of distal colons were prepared as described above and were incubated with HCl 2 M at 37°C for 10 min for permeabilization. Blocking was then made using normal goat serum (Biological Industries) for 1 h in room temperature. Tissues were incubated at 4°C overnight with rat polyclonal antibodies against BrdU (1 : 400) (Sigma-Aldrich) and then 1 h at room temperature with anti- rat IgG (1 : 100) fluorescently labelled with Cy3 (Jackson ImmunoResearch). On some of the tissues, we used DAPI-containing immunomount solution (DAPI Fluoromount-G, Southern Biotech). Images were taken using a florescence microscope at 20× magnification. Number of BrdU-stained cells were counted and normalized to the number of crypts (as seen using bright-field microscopy) in the same area.

(g) Statistical analysis

Data are expressed as mean ± s.e.m. Statistical significance between groups were analysed by ANOVA multiple variables test, followed by Tukey–Kramers post-hoc test using the STATISTIC program, or Student's *T*-test as appropriate.

3. Results

(a) Znr/GPR39 triggers metabotropic Ca^{2+} signalling and upregulates occludin expression in Caco-2 colonocytes

We first asked if ZnR/GPR39 triggers metabotropic Ca^{2+} signalling in colonocytes. Application of Zn^{2+} (200 µM) to Caco-2 cells loaded with the Ca^{2+} indicator Fura-2 triggered

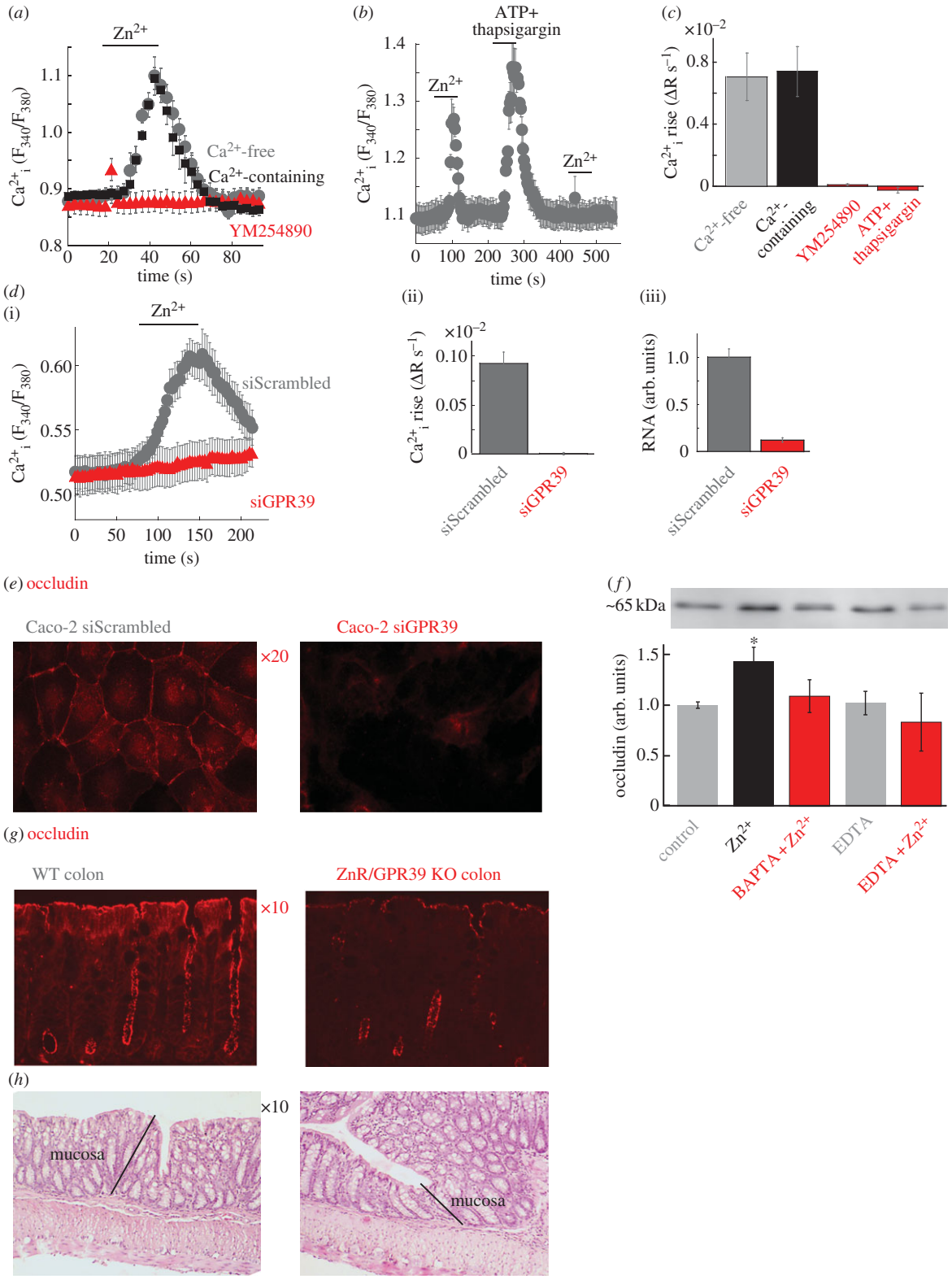

Figure 1. ZnR/GPR39 triggers Ca^{2+} signalling in Caco-2 colonocytes and regulates occludin expression. (*a*) Caco-2 colonocytes were loaded with Fura-2 and responses were monitored in Ringer's solution with (grey) and without (black) Ca^{2+}-free following the addition of Zn^{2+} (200 µM) to control cell or cells treated with the Gq inhibitor YM254890 (1 µM). Averaged response from seven cells in one slide is shown. (*b*) The response to Zn^{2+} (200 µM, as in *a*) was monitored before or after Ca^{2+} store depletion (ATP 100 µM+thapsigargin 200 nM). (*c*) The average initial rate of the Ca^{2+} response as monitored in (*a*,*b*) ($n = 10$). (*d*) The response to Zn^{2+} (200 µM, as in *a*) was monitored in Caco-2 cells treated with an siRNA construct aimed to silence ZnR/GPR39 (siGPR39) or a scrambled control (siScrambled). Panel (ii) shows the average rate of initial Ca^{2+} response ($n = 20$), panel (iii) shows mRNA level in control or siGPR39 silenced cells ($n = 3$). (*e*) Representative immunofluorescence analysis of the expression of the tight junction protein occludin in siScrambled or siGPR39 Caco-2 cells. (*f*) Analysis of occludin expression level after Ca^{2+} depletion (see Material and methods) in differentiated Caco-2 cells treated with Zn^{2+} (200 µM) or without it (control) in the presence of the intracellular Ca^{2+} chelator BAPTA-AM (5 µM) or the non-permeable Ca^{2+} chelator EDTA (100 µM) ($n = 2$, $^*p < 0.05$). (*g*) Representative immunofluorescence analysis of the expression of the tight junction protein occludin in colon tissue from WT or ZnR/GPR39 KO mice. (*h*) Histochemical (H&E) analysis of colon tissue sections from WT and ZnR/GPR39 KO mice in sections of colon. The mucosa layer is marked, showing similar crypt formation and low extent of inflammation in both genotypes.

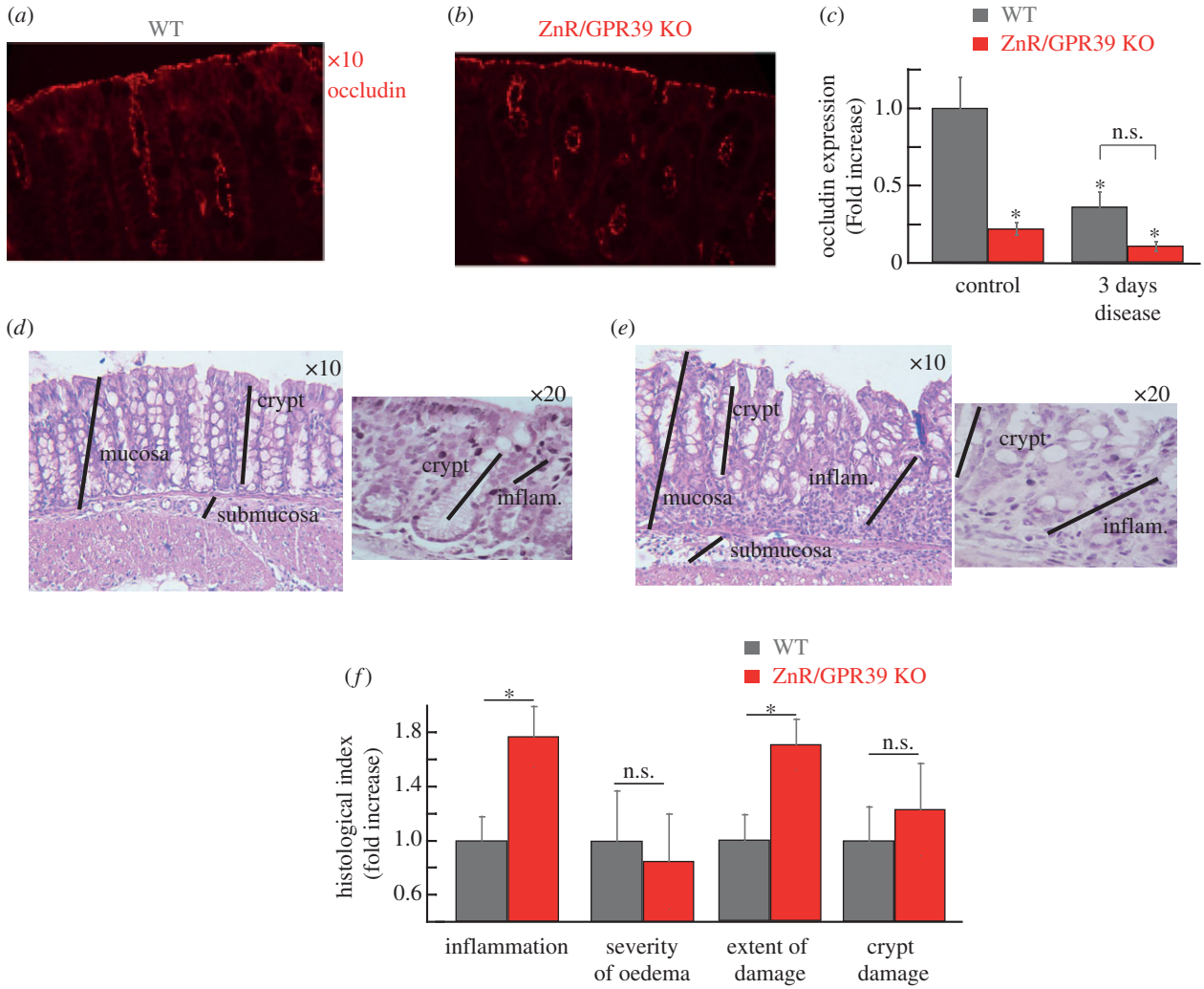

Figure 2. Clinical and histological analysis of colon tissue at the acute phase of DSS treatment. (*a*,*b*) Representative immunofluorescence analysis of the expression of the tight junction protein occludin in colon tissue from WT or ZnR/GPR39 KO mice following 3 days DSS treatment. (*c*) Quantification of occludin expression levels during basal (figure 1*f*) or disease condition (figure 2*a*) using a threshold analysis (see Material and methods). Results were normalized to the average count in the WT group at baseline/control conditions ($n = 15-35$ slices from six to eight mice for each treatment, $^*p < 0.05$ compared to control WT). (*d*,*e*) H&E analysis of colon tissue sections from WT and ZnR/GPR39 KO mice in sections of colon following 3 days DSS treatment. The black lines mark the mucosal layer, intact crypts in the mucosa or the inflamed mucosal layer (inflam). (*f*) Histological evaluation along the colon was done to obtain indices of: the inflammation level, severity of oedema, extent of inflamed tissue within the wall (extent of damage) and crypt damage (see Material and methods). Each of the indices is normalized to the level in WT tissues. ($n = 22-23$ per genotype, $^*p < 0.05$ compared to WT).

a robust response in the absence or the presence of extracellular Ca^{2+} (figure 1*a*,*c*). This response was completely eliminated by the selective Gαq inhibitor, YM254890 [28,29], suggesting that it is mediated by the IP3 pathway. We then depleted intracellular Ca^{2+} stores by applying ATP (100 µM), which activates the purinergic receptor to release Ca^{2+} from the stores, together with thapsigargin (200 nM) that inhibits the SERCA and blocks replenishment of the Ca^{2+} stores [30]. The Zn^{2+}-dependent Ca^{2+} response was abolished following depletion of intracellular Ca^{2+} stores (figure 1*b*,*c*), indicating that Zn^{2+} activates metabotropic Ca^{2+} signalling in Caco-2 colonocytes. Importantly, the intracellular Ca^{2+} response was also abolished when ZnR/GPR39 was silenced using an siRNA construct (figure 1*d*), indicating that it is directly mediated by ZnR/GPR39. To determine a physiological role for ZnR/GPR39-dependent Ca^{2+} signalling, we asked whether ZnR/GPR39 regulates the expression of occludin, an important factor of the tight junction barrier in the colon [3]. Indeed, silencing of ZnR/GPR39 in Caco-2 cells largely downregulated occludin expression (figure 1*e*). Next we asked if ZnR/GPR39-dependent Ca^{2+} signalling is essential for regulating occludin expression. Caco-2 cells were differentiated thus forming tight junctions, and Ca^{2+} was then removed from the growth medium for 16 h to lower occludin expression [23]. Activation of ZnR/GPR39 by Zn^{2+} (200 µM) largely enhanced the recovery of occludin expression compared with control cells not treated with Zn^{2+} (figure 1*f*). The Zn^{2+}-dependent occludin expression was abolished when Ca^{2+} signalling was inhibited by the intracellular Ca^{2+} chelator BAPTA, or when extracellular Zn^{2+} was chelated by EDTA (100 µM). Thus, our results indicate that ZnR/GPR39, via activation of intracellular Ca^{2+} signals, enhances recovery of occludin expression.

We therefore asked whether ZnR/GPR39 may also affect the expression of occludin *in vivo*. Expression of the tight junction protein occludin was fourfold lower in mice lacking ZnR/GPR39 (ZnR/GPR39 KO) compared with WT mice (figure 1*g*). Histological analysis of HE-stained colon tissues indicated that mucosal/submucosal organization was similar in both genotypes, crypts were intact and no oedema or excessive inflammatory cells were seen in both genotypes (figure 1*h*).

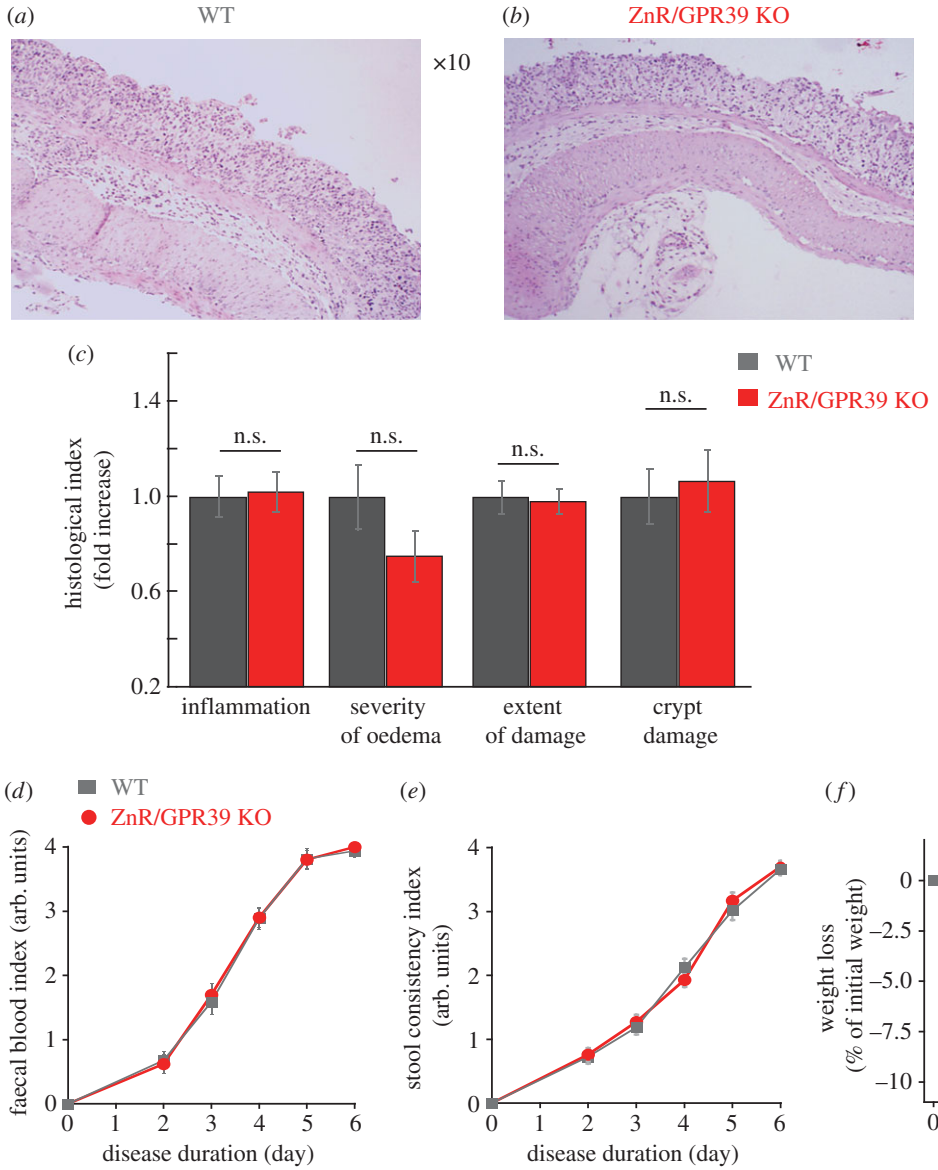

Figure 3. Clinical and histological analysis of colon tissue at the acute phase of DSS treatment. (*a*,*b*) Representative HE-stained colon tissue sections obtained following 6 days of DSS treatment from WT (*a*) and ZnR/GPR39 KO (*b*). (*c*) Histological evaluation along the colon, performed as described in figure 1, shows no significant differences in the severity of the injury to WT and ZnR/GPR39 KO mice. (*d*) Faecal blood and (*e*) faecal consistency indices were monitored during the 6 days of DSS treatment ($n = 22-23$, per genotype). The scores for blood index and stool consistency were between 0 and 4, when 0 indicates the healthy stage (see Material and methods). (*f*) Weight loss during DSS treatment is shown. During the first 2 days of DSS treatment, the weight of treated mice increased by $0.6 \pm 0.4\%$ in WT mice and $1.5 \pm 0.4\%$ in ZnR/GPR39 KO mice ($n = 22-23$, per genotype).

(b) Acute colitis phase: DSS treatment

To determine whether the impaired Ca^{2+} signalling and epithelial barrier, in the absence of ZnR/GPR39, results in enhanced susceptibility to inflammatory disease we employed the DSS-induced acute colitis model [31]. Substantial decreases in occludin levels were observed in WT tissues after 3 days of DSS treatment compared with the untreated controls (figure 2*a*). No change was observed in occludin expression level in ZnR/GPR39 KO mice (figure 2*b*), consistent with the very low basal occludin expression levels. Importantly, 3 days of DSS treatment attenuate occludin expression in WT mice, reducing it to the level monitored in ZnR/GPR39 KO mice already under basal conditions (figure 2*c*). Histological analysis of colon tissue sections on the thirrd day of DSS treatment indicated that tissue organization was still preserved in WT tissues but much less preserved in ZnR/GPR39 KO (figure 2*d*–*e*). Moreover, inflammation was almost absent in the WT tissue (figure 2*d*) while regions containing infiltrating inflammatory cells within the mucosa of ZnR/GPR39 KO mice were observed (figure 2*e*). For quantifying mucosal integrity, we analysed four features along the colon: level of inflammation, severity of oedema, extent of tissue damage within the wall and extent of crypt damage (Material and methods). Following 3 days of DSS treatment, the level of inflammation and the extent of tissue damage indices were significantly higher in ZnR/GPR39 KO (inflammation: 3.6 ± 0.4; extent: 2.8 ± 0.3) compared with WT (inflammation: 2.0 ± 0.4; extent: 1.6 ± 0.3; $p < 0.05$) mice (figure 2*f*, note that for simplicity of presentation indices are normalized to WT in the bar graphs). These findings indicate that in ZnR/GPR39 KO tissue the destruction of the epithelial layer was almost complete, while this layer was partially preserved in WT mice, as reflected by the larger extent of tissue damage (figure 2*f*). Moreover, crypt shortening was observed in both genotypes but loss of crypts was more severe in the ZnR/GPR39 KO mice in some regions along the colon

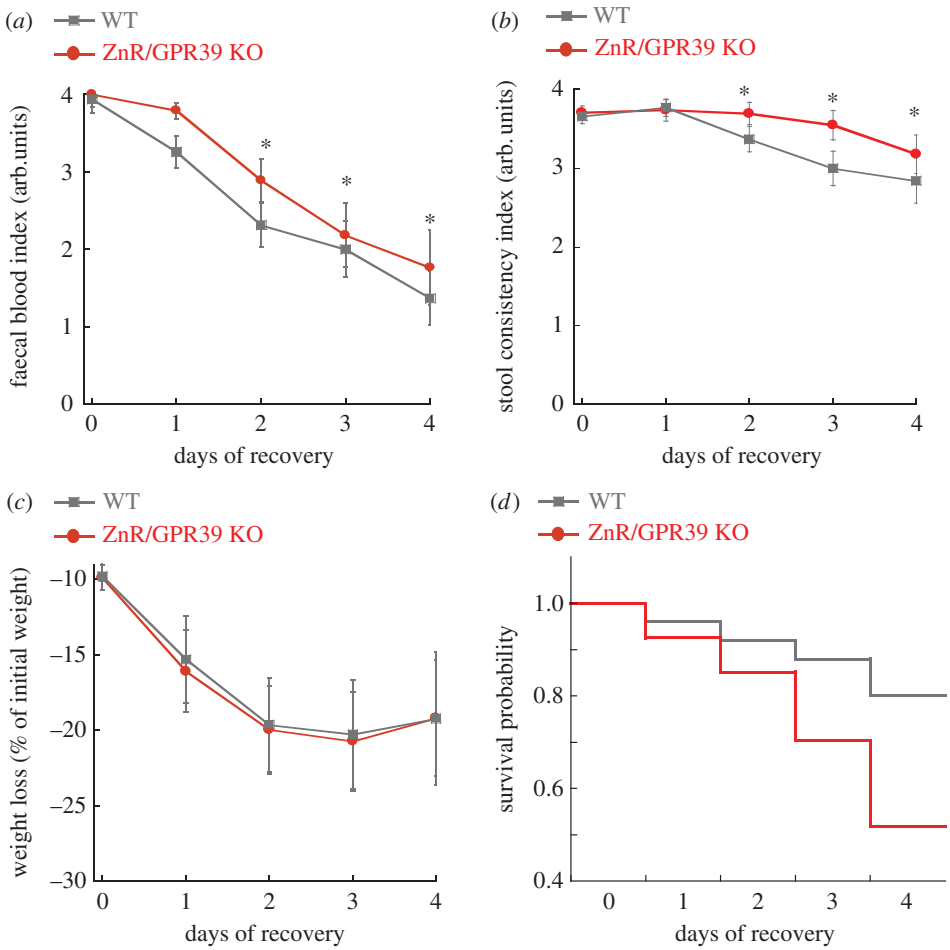

Figure 4. ZnR/GPR39 ameliorates clinical symptoms of the disease and enhances survival during recovery from DSS treatment. Clinical scores were monitored daily during the recovery period, following removal of DSS treatment, while on a regular drinking regime. Day 0 is the 6th day of DSS and shows the data as figure 3. (*a*) Faecal blood and (*b*) stool consistency indices as well as (*c*) weight loss were determined in WT versus ZnR/GPR39 KO mice (as in figure 3 and Material and methods). (*d*) Survival probability during the recovery period is presented using the Kaplan–Maier plot, $p < 0.05$ between WT and ZnR/GPR39 KO mice.

length. In agreement with the major effect on the epithelial layer, WT mice were more resistant to the inflammatory response in the mucosal layer. On day 6 of DSS treatment, histological scores showed complete loss of crypts, focal ulcerations, severe infiltration of inflammatory cells to the mucosa and severe oedema in the submucosa (figure 3*a–c*). Importantly, there were no differences between the WT and the ZnR/GPR39 KO tissues following 6 days of DSS treatment. The tissues exhibit nearly complete erosion of the epithelial layer throughout the length of the colon. Note that ZnR/GPR39 activity was monitored in colonocytes (figure 1), which were similarly absent in both genotypes on the 6th day of DSS treatment. Clinical parameters were also determined throughout the 6 days of DSS treatment (Material and methods). Changes in haemoccult positivity, gross bleeding, stool consistency and weight were monitored daily. We observed no significant differences between WT and ZnR/GPR39 KO mice in all parameters during all 6 days of DSS treatment, disease phase (figure 3*d–f*). Previous studies indicated that clinical manifestations during the acute disease phase do not necessarily reflect the histological severity of the disease in the colon tissue [32], in agreement with our results. Because the clinical and histopathological scores were similar between the genotypes on the 6th day of DSS treatment, we continued to study whether ZnR/GPR39 affects a recovery phase, following removal of DSS.

(c) Recovery phase: following DSS removal

The mice were allowed to recover by removing DSS from their drinking water, yielding a period that bears resemblance to the remission period in IBD patients [33]. Analysis of clinical symptoms revealed that WT mice showed significantly faster decrease in faecal blood indices (figure 4*a*) and watery stool consistency (figure 4*b*) compared with ZnR/GPR39 KO mice, although both genotypes continued to lose weight even following the removal of DSS (figure 4*c*). These differences were seen on the second day of the recovery period and remained statistically significant even after 4 days, indicating a more rapid recovery of WT compared to ZnR/GPR39 KO mice. In addition, ZnR/GPR39 KO mice had lower overall survival probability compared with WT mice (figure 4*d*, Kaplan–Meier probability $p < 0.05$), averaged daily mortality rate during the recovery period was $14 \pm 1\%$ in ZnR/GPR39 KO compared to $7.5 \pm 0.5\%$ in WT ($p < 0.05$). Thus, during the recovery from DSS-induced colitis, clinical symptoms were ameliorated in WT mice compared to ZnR/GPR39 KO mice.

Histological analysis of distal colon tissue sections on day 2 of the recovery (figure 5*a–b*) showed no significant differences between the genotypes in the extent of tissue damage within the colon wall (4.3 ± 0.1 in WT versus 4.5 ± 0.2 in ZnR/GPR39 KO). This finding is consistent with the severe acute response triggered following destruction of the epithelial layer during 6 days of toxin treatment in both genotypes.

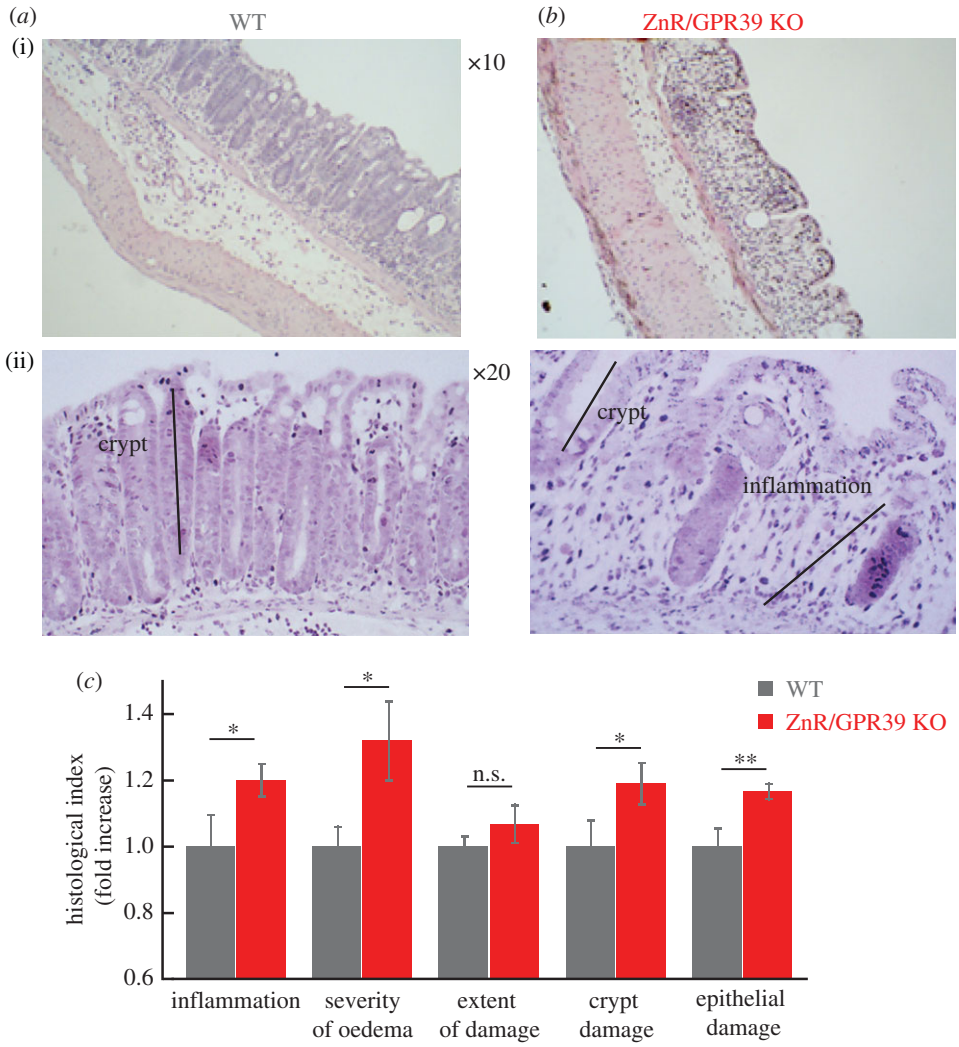

Figure 5. ZnR/GPR39 promotes crypts regeneration during the recovery period. (*a*,*b*) Representative HE-stained colon tissues from WT (*a*) and ZnR/GPR39 KO (*b*) mice obtained on the second day of the recovery phase. (*c*) Histological evaluation along the colon was done to obtain indices of: the inflammation level, severity of oedema, extent of inflamed tissue within the wall (extent of damage), crypt damage and extent of epithelial damage (regions of destructed tissue along the epithelial layer). For clarity of presentation in a bar graph, each of the indices is normalized to the level in WT tissues. ($n = 28-30$ per genotype, $^*p < 0.05$ compared to WT).

By contrast, the indices for immune cells infiltration (inflammation index of 9.0 ± 0.9 in WT versus 10.8 ± 0.4 in ZnR/GPR39 KO; $p < 0.05$) and the severity of oedema (4.5 ± 0.3 in WT versus 6.0 ± 0.5 in ZnR/GPR39 KO; $p < 0.05$) were significantly higher in tissues from ZnR/GPR39 KO mice compared with WT, suggesting partial recovery of the inflammatory response in WT but not in the ZnR/GPR39 KO mice. Importantly, the crypt damage index, reflecting the direct loss of crypts along the colon, was significantly higher in the ZnR/GPR39 KO (13.9 ± 0.7 in ZnR/GPR39 KO versus 11.7 ± 0.9 in WT; $p < 0.05$). In addition, the index of epithelial damage was significantly higher in ZnR/GPR39 KO mice compared with WT (15.5 ± 0.3 in ZnR/GPR39 KO versus 13.3 ± 0.7 in WT; $p < 0.01$). As such, in tissue from ZnR/GPR39 KO mice we observed fewer and relatively short crypts with scarce regions covered by surface epithelium, indicating mild regeneration from the destruction by DSS. But, in tissue from WT mice we observed more regions along the colon where the surface epithelial layer recovered from the damage and substantial numbers of crypts were regenerated already 2 days following removal of DSS (figure 5*a*–*c*, note that indices in *c* are normalized to WT).

We then monitored BrdU incorporation, as an *in situ* proliferative marker, to study if the differences in epithelial recovery between WT and ZnR/GPR39 KO are directly linked to proliferation. Quantitative analysis was done by counting the number of BrdU-stained cells per crypt (as observed under bright-field microscopy of the same field of view). Slices from the distal colon were obtained from control mice, before DSS treatment (control) to determine whether ZnR/GPR39 KO mice have slower proliferation rates in the normal tissue. In control tissues, under basal conditions, we did not monitor differences in proliferating colonocytes between genotypes, showing 2.7 ± 0.3 cells crypt^{-1} in WT mice and 2.8 ± 0.2 cell crypt^{-1} in ZnR/GPR39 KO mice (figure 6*a* left panels and *b*). This is important because it allows us to determine whether the proliferation rates are changed under conditions of recovery from the injury when this process plays an important role in tissue repair. We then studied the differences in proliferation rates on the second and fourth days of the recovery period (figure 6*a*–*b*). On the second day of the recovery period, crypt cell proliferation among WT mice dramatically increased compared with control mice untreated with DSS (4.8 ± 0.3 cells crypt^{-1}, $p < 0.05$ compared to control, figure 5*a*(i)), indicating

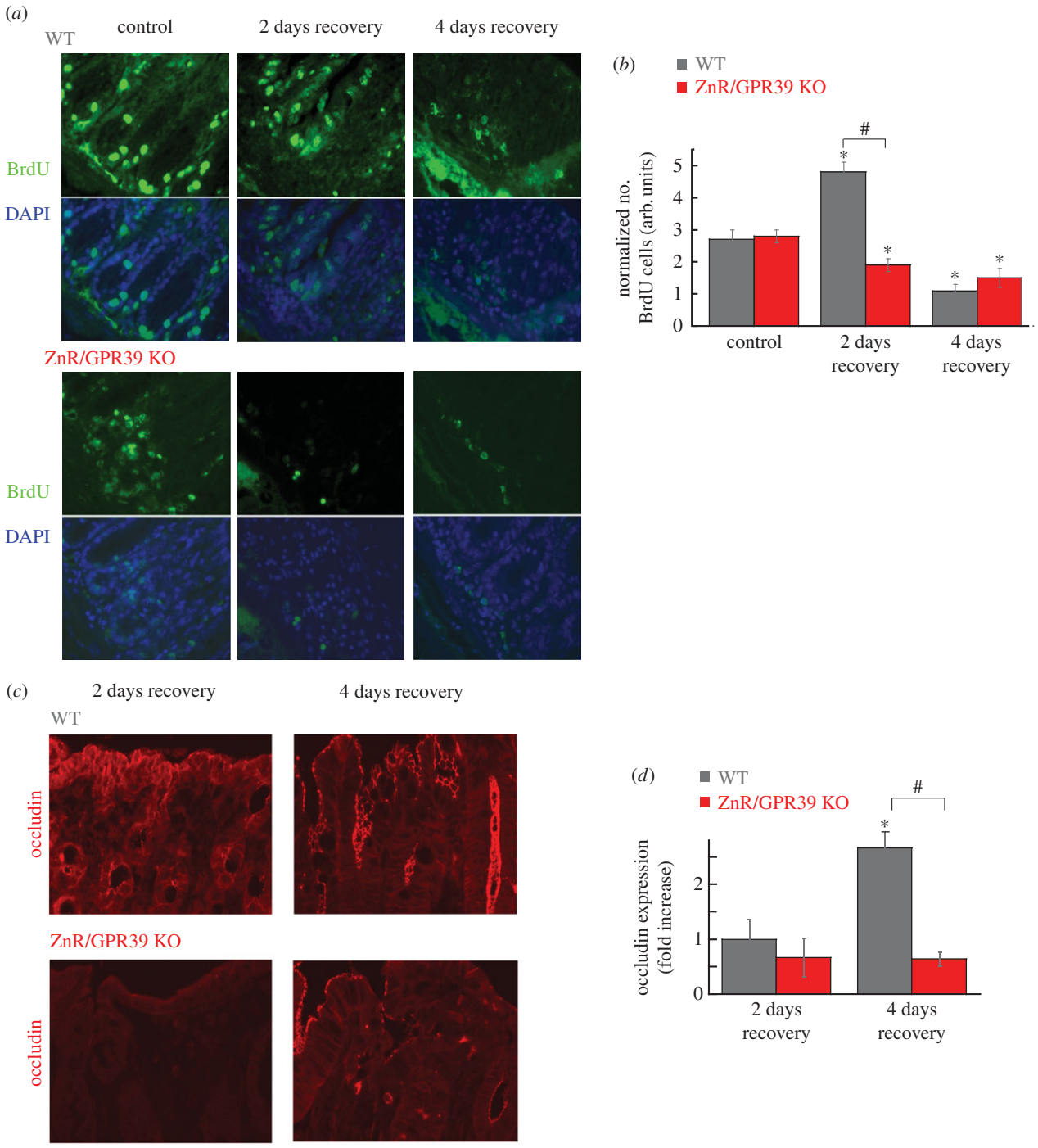

Figure 6. ZnR/GPR39 promotes cell proliferation. (*a*) Representative BrdU-stained tissues of WT or ZnR/GPR39 KO colon from control (non-treated) mice or following DSS treatment at 2 days or 4 days of the recovery period (×20). DAPI staining was added as a control. Note that DAPI staining is seen in epithelial as well as in inflammatory cells nuclei within the mucosa. (*b*) Analysis of epithelial proliferation, using BrdU-stained tissue, comparing the number of stained cells to the number of crypts observed in a field. ($n = 37$ per genotype, $^{*}p < 0.05$ compared to control WT, $^{\#}p < 0.05$, between WT and ZnR/GPR39 KO on day 2 of recovery). (*c*) Representative images of occludin expression levels during the recovery period, on the second and fourth days following removal of DSS, recovery phase. (*d*) Quantitative analysis was performed as in figure 1 ($n = 10-30$ slices from 6 to 10 mice from each treatment and each genotype, $^{*}p < 0.05$ compared to 2 days of recovery in WT, $^{\#}p < 0.05$ compared to 4 days of recovery in WT).

that proliferation of epithelial cells is accelerated, apparently to facilitate repair of the injured epithelial layer. In striking contrast to the WT colon, in ZnR/GPR39 KO mice the proliferation within regenerated crypts during the recovery phase from DSS was not enhanced, and even decreased compared with untreated mice (1.9 ± 0.2 cells crypt^{-1}, $p < 0.05$, figure 6*a* bottom panels). BrdU-stained cells were counted only in crypts that had well-defined morphology and structure, and therefore this parameter reflects cell proliferation rates in preserved/renewed crypts and argues against this being a result of the general larger damage of the epithelial layer seen in ZnR/GPR39 KO mice. After 4 days of recovery, proliferation rate in WT mice decreased to 1.1 ± 0.2 cells crypt^{-1}, suggesting a shift to a differentiation phase. Yet, in tissues from ZnR/GPR39 KO mice, even on the fourth day of recovery, the number of BrdU-stained cells remained low at 1.5 ± 0.3 cells crypt^{-1}. Thus, in WT mice we monitored a large increase in rates of proliferation during the initial recovery, thereby rapidly renewing the epithelial layer. By contrast, in ZnR/GPR39 KO mice we observed attenuated epithelial

proliferation even during the recovery period. These results suggest that ZnR/GPR39 is required for promoting proliferation during the recovery phase following epithelial erosion but not during the basal state, when proliferating cell numbers were similar in the presence or the absence of the receptor.

Differentiation and formation of tight junctions are further essential for the complete recovery of epithelial barrier [34], thus we compared the expression levels of occludin during the recovery period. In colon sections from the second day of recovery, when peak proliferation was monitored, WT and ZnR/GPR39 KO mice still exhibit low levels of occludin expression. Importantly, on the fourth day of recovery, occludin levels were increased in WT mice, by about threefold, compared to the second day (figure 6*c–d*). By contrast, occludin expression in ZnR/GPR39 KO mice did not change from day 2 to day 4 of the recovery period (figure 6*c*,*d*). Altogether our results suggest that ZnR/GPR39 expression is required for the formation and function of the tight epithelial barrier during DSS-induced colitis and the recovery period.

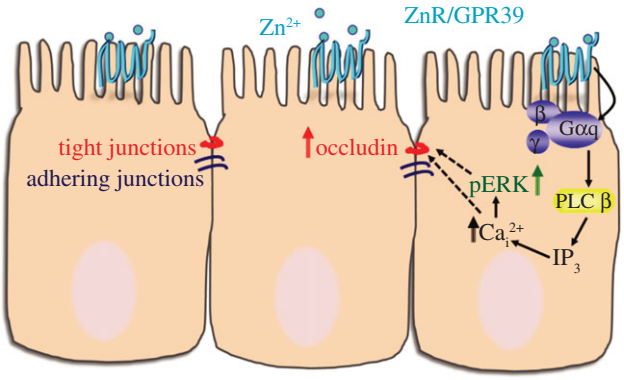

Figure 7. Scheme of ZnR/GPR39 signalling activated by Zn^{2+} to enhance tight junction formation. Our results indicate that ZnR/GPR39 signalling activates Ca^{2+} release from thapsigargin-dependent endoplasmic reticulum stores in colonocytes, thereby upregulating occludin expression. *In vivo*, ZnR/GPR39 expression is essential to enhance the recovery of occludin expression and colonocytes proliferation following barrier disruption by DSS.

4. Discussion

Reduction in the expression of occludin was seen in inflamed epithelia of both Crohn's disease and ulcerative colitis patients even at early stages of the disease [35]. A fundamental difference between WT and ZnR/GPR39 KO mice is the basal expression of occludin, in the absence of any pathological condition. Compromised epithelial barrier in the absence of ZnR/GPR39 may hence increase epithelial permeability. Indeed, during the disease phase (DSS treatment), colon tissue from ZnR/GPR39 KO mice exhibited more damage compared with WT. Moreover, enhanced faecal expulsion and accelerated gastric emptying that were described in ZnR/GPR39 KO mice [22] may also result from the low expression of occludin and compromised tight junction barrier. The low susceptibility to DSS during the disease phase may result from the severity of the chemical DSS insult which damages the epithelial layer. However, the effect of the receptor is fully manifested during the recovery when epithelial cells expressing ZnR/GPR39 enhance the buildup of the epithelial layer and barrier function. Thus, our results suggest that ZnR/GPR39 has an important role in rebuilding the epithelial barrier during remission in ulcerative disease (figure 7).

Consistent with the findings in this study, extracellular Zn^{2+} activates ZnR/GPR39 leading to Ca^{2+} signalling and activating epithelial proliferation and migration [18–20,36,37]. The ZnR/GPR39 response is mediated via the IP3 pathway and induces release of intracellular Ca^{2+}, which is essential for downstream signalling [38] and recovery of occludin expression. Remarkably, ZnR/GPR39-dependent colon epithelial cell proliferation was largely increased only during the recovery period, promoting epithelial renewal following its erosion during the disease phase. Interestingly, the Zn^{2+} transporter Zip14 has been recently shown to regulate occludin expression [39]. Further studies will be required to study the interaction of ZnR/GPR39 and intracellular Zn^{2+} transporters in regulating proliferation and differentiation.

One could argue that ZnR/GPR39 may have a direct role on the immune response, as it is well known that zinc deficiency affects immune system cells resulting in higher susceptibility to infections [40–42]. Our results, however, suggest a prominent role for ZnR/GPR39-dependent regulation of the epithelial barrier as the pathway for attenuating the DSS-induced response. Consistent with this hypothesis, the inflammatory index was lower in WT mice during the DSS-induced disease phase when ZnR/GPR39 was functional on WT epithelial cells. By contrast, when erosion of the epithelial layer was complete (sixth day of DSS) we found no differences in the inflammatory response between genotypes. Indeed, zinc supplementation to Crohn's disease patients during clinical remission reduced intestinal permeability [12]. A similar role on epithelial barrier, and thereby permeability, was described for Zn^{2+} in lung bacterial infection [43]. Importantly, a direct effect of ZnR/GPR39 on the epithelial barrier is also supported by the faster renewal of the epithelial surface layer along the mucosa with crypt reorganization and increased proliferation rate of epithelial cells in WT compared with ZnR/GPR39 KO mice. The enhanced recovery of the epithelial barrier in WT mice was reflected by amelioration of the clinical symptoms (faecal blood and diarrhoea) during the recovery phase in the WT mice compared to ZnR/GPR39 KO.

The essential role of zinc for function of the digestive system is documented in many studies [7,10,13,44], but as the specific molecular targets of this ion are unknown the regime of treatment is controversial. By identifying a molecular target of Zn^{2+} in the digestive tract, ZnR/GPR39, we provide a tool to study the effects of zinc treatment in IBD in a controllable manner. To date, there is no known medical cure for IBD that targets the epithelial layer, we show that ZnR/GPR39 directly promotes intestinal barrier formation and function and may therefore provide an effective therapeutic target in ulcerative diseases.

Ethics. Experimental procedures were performed in accordance with a protocol approved by the committee for the Ethical Care and Use of Animal in Experiments at the Faculty of Health Science at Ben-Gurion University of the Negev.

Authors' contributions. L.S., M.M. and L.C. performed experiments, analysed data and wrote the manuscript; I.S. conceived and wrote the manuscript; M.H. conceived and planned the experiments, analysed data and wrote the manuscript.

Competing interests. We have no competing interests to declare.

Funding. This work was supported by the Israel Science Foundation (grant no. 978/13 to M.H.).

Acknowledgements. The GPR39 KO mice were kindly provided by D. Moechars from Johnson & Johnson Pharmaceutical Research and Development, a Division of Janssen Pharmaceutica. We thank Elena Voronov for technical help with the DSS model.

References

1. Danese S, Fiocchi C. 2011 Ulcerative colitis. *N. Engl. J. Med.* **365**, 1713–1725. (doi:10.1056/NEJMra1102942)
2. Hering NA, Fromm M, Schulzke JD. 2012 Determinants of colonic barrier function in inflammatory bowel disease and potential therapeutics. *J. Physiol.* **590**, 1035–1044. (doi:10.1113/jphysiol.2011.224568)
3. Dorfel MJ, Huber O. 2012 Modulation of tight junction structure and function by kinases and phosphatases targeting occludin. *J. Biomed. Biotechnol.* **2012**, 807356. (doi:10.1155/2012/807356)
4. Bertiaux-Vandaele N *et al.* 2011 The expression and the cellular distribution of the tight junction proteins are altered in irritable bowel syndrome patients with differences according to the disease subtype. *Am. J. Gastroenterol.* **106**, 2165–2173. (doi:10.1038/ajg.2011.257)
5. Su L *et al.* 2013 TNFR2 activates MLCK-dependent tight junction dysregulation to cause apoptosis-mediated barrier loss and experimental colitis. *Gastroenterology* **145**, 407–415. (doi:10.1053/j.gastro.2013.04.011)
6. Scrimgeour AG, Lukaski HC. 2008 Zinc and diarrheal disease: current status and future perspectives. *Curr. Opin. Clin. Nutr. Metab. Care* **11**, 711–717. (doi:10.1097/MCO.0b013e3283109092)
7. Goh J, O'Morain CA. 2003 Review article: nutrition and adult inflammatory bowel disease. *Aliment Pharmacol. Ther.* **17**, 307–320. (doi:10.1046/j.1365-2036.2003.01482.x)
8. Kulkarni H, Mamtani M, Patel A. 2012 Roles of zinc in the pathophysiology of acute diarrhea. *Curr. Infect. Dis. Rep.* **14**, 24–32. (doi:10.1007/s11908-011-0222-8)
9. Walker CL, Black RE. 2010 Zinc for the treatment of diarrhoea: effect on diarrhoea morbidity, mortality and incidence of future episodes. *Int. J. Epidemiol.* **39**(Suppl. 1), i63–i69. (doi:10.1093/ije/dyq023)
10. Sikora SK, Spady D, Prosser C, El-Matary W. 2011 Trace elements and vitamins at diagnosis in pediatric-onset inflammatory bowel disease. *Clin. Pediatr.* **50**, 488–492. (doi:10.1177/0009922810397041)
11. Ojuawo A, Keith L. 2002 The serum concentrations of zinc, copper and selenium in children with inflammatory bowel disease. *Cent. Afr. J. Med.* **48**, 116–119.
12. Sturniolo GC, Di Leo V, Ferronato A, D'Odorico A, D'Inca R. 2001 Zinc supplementation tightens 'leaky gut' in Crohn's disease. *Inflamm. Bowel Dis.* **7**, 94–98. (doi:10.1097/00054725-200105000-00003)
13. Sturniolo GC, Fries W, Mazzon E, Di Leo V, Barollo M, D'Inca R. 2002 Effect of zinc supplementation on intestinal permeability in experimental colitis. *J. Lab. Clin. Med.* **139**, 311–315. (doi:10.1067/mlc.2002.123624)
14. Finamore A, Massimi M, Conti Devirgiliis L, Mengheri E. 2008 Zinc deficiency induces membrane barrier damage and increases neutrophil transmigration in Caco-2 cells. *J. Nutr.* **138**, 1664–1670.
15. Luk HH, Ko JK, Fung HS, Cho CH. 2002 Delineation of the protective action of zinc sulfate on ulcerative colitis in rats. *Eur. J. Pharmacol.* **443**, 197–204. (doi:10.1016/S0014-2999(02)01592-3)
16. Hershfinkel M, Moran A, Grossman N, Sekler I. 2001 A zinc-sensing receptor triggers the release of intracellular Ca^{2+} and regulates ion transport. *Proc. Natl Acad. Sci. USA* **98**, 11 749–11 754. (doi:10.1073/pnas.201193398)
17. Hershfinkel M, Silverman WF, Sekler I. 2007 The zinc sensing receptor, a link between zinc and cell signaling. *Mol. Med.* **13**, 331–336. (doi:10.2119/2006-00038.Hershfinkel)
18. Sharir H, Zinger A, Nevo A, Sekler I, Hershfinkel M. 2010 Zinc released from injured cells is acting via the Zn^{2+}-sensing receptor, ZnR, to trigger signaling leading to epithelial repair. *J. Biol. Chem.* **285**, 26 097–26 106. (doi:10.1074/jbc.M110.107490)
19. Cohen L, Azriel-Tamir H, Arotsker N, Sekler I, Hershfinkel M. 2012 Zinc sensing receptor signaling, mediated by GPR39, reduces butyrate-induced cell death in HT29 colonocytes via upregulation of clusterin. *PLoS ONE* **7**, e35482. (doi:10.1371/journal.pone.0035482)
20. Cohen L, Sekler I, Hershfinkel M. 2014 The zinc sensing receptor, ZnR/GPR39, controls proliferation and differentiation of colonocytes and thereby tight junction formation in the colon. *Cell Death Dis.* **5**, e1307. (doi:10.1038/cddis.2014.262)
21. Popovics P, Stewart AJ. 2011 GPR39: a Zn^{2+}-activated G protein-coupled receptor that regulates pancreatic, gastrointestinal and neuronal functions. *Cell Mol. Life Sci* **68**, 85–95. (doi:10.1007/s00018-010-0517-1)
22. Moechars D *et al.* 2006 Altered gastrointestinal and metabolic function in the GPR39-obestatin receptor-knockout mouse. *Gastroenterology* **131**, 1131–1141. (doi:10.1053/j.gastro.2006.07.009)
23. Stuart RO, Sun A, Panichas M, Hebert SC, Brenner BM, Nigam SK. 1994 Critical role for intracellular calcium in tight junction biogenesis. *J. Cell Physiol.* **159**, 423–433. (doi:10.1002/jcp.1041590306)
24. Mahler M, Bristol IJ, Leiter EH, Workman AE, Birkenmeier EH, Elson CO, Sundberg JP. 1998 Differential susceptibility of inbred mouse strains to dextran sulfate sodium-induced colitis. *Am. J. Physiol.* **274**, G544–G551.
25. Cooper HS, Murthy SN, Shah RS, Sedergran DJ. 1993 Clinicopathologic study of dextran sulfate sodium experimental murine colitis. *Lab. Invest.* **69**, 238–249.
26. Gramlich T, Petras RE. 2007 Pathology of inflammatory bowel disease. *Semin. Pediatr. Surg.* **16**, 154–163. (doi:10.1053/j.sempedsurg.2007.04.005)
27. Kim CJ, Kovacs-Nolan J, Yang C, Archbold T, Fan MZ, Mine Y. 2009 L-cysteine supplementation attenuates local inflammation and restores gut homeostasis in a porcine model of colitis. *Biochim. Biophys. Acta* **1790**, 1161–1169. (doi:10.1016/j.bbagen.2009.05.018)
28. Sharir H, Hershfinkel M. 2005 The extracellular zinc-sensing receptor mediates intercellular communication by inducing ATP release. *Biochem. Biophys. Res. Commun.* **332**, 845–852. (doi:10.1016/j.bbrc.2005.05.036)
29. Takasaki J, Saito T, Taniguchi M, Kawasaki T, Moritani Y, Hayashi K, Kobori M. 2004 A novel Galphaq/11-selective inhibitor. *J. Biol. Chem.* **279**, 47 438–47 445. (doi:10.1074/jbc.M408846200)
30. Cummins MM, O'Mullane LM, Barden JA, Cook DI, Poronnik P. 2000 Purinergic responses in HT29 colonic epithelial cells are mediated by G protein alpha -subunits. *Cell Calcium* **27**, 247–255. (doi:10.1054/ceca.2000.0120)
31. Kim HS, Berstad A. 1992 Experimental colitis in animal models. *Scand. J. Gastroenterol.* **27**, 529–537. (doi:10.3109/00365529209000116)
32. Perse M, Cerar A. 2012 Dextran sodium sulphate colitis mouse model: traps and tricks. *J. Biomed. Biotechnol.* **2012**, 718617. (doi:10.1155/2012/718617)
33. Rose 2nd , WA, Sakamoto K, Leifer CA. 2012 Multifunctional role of dextran sulfate sodium for *in vivo* modeling of intestinal diseases. *BMC Immunol.* **13**, 41. (doi:10.1186/1471-2172-13-41)
34. Forster C. 2008 Tight junctions and the modulation of barrier function in disease. *Histochem. Cell Biol.* **130**, 55–70. (doi:10.1007/s00418-008-0424-9)
35. Bruewer M, Samarin S, Nusrat A. 2006 Inflammatory bowel disease and the apical junctional complex. *Ann. NY Acad. Sci.* **1072**, 242–252. (doi:10.1196/annals.1326.017)
36. Asraf H, Salomon S, Nevo A, Sekler I, Mayer D, Hershfinkel M. 2014 The ZnR/GPR39 interacts with the CaSR to enhance signaling in prostate and salivary epithelia. *J. Cell Physiol.* **229**, 868–877. (doi:10.1002/jcp.24514)
37. Dubi N, Gheber L, Fishman D, Sekler I, Hershfinkel M. 2008 Extracellular zinc and zinc-citrate, acting through a putative zinc-sensing receptor, regulate growth and survival of prostate cancer cells. *Carcinogenesis* **29**, 1692–1700. (doi:10.1093/carcin/bgn027)

38. Azriel-Tamir H, Sharir H, Schwartz B, Hershfinkel M. 2004 Extracellular zinc triggers ERK-dependent activation of Na^+/H^+ exchange in colonocytes mediated by the zinc-sensing receptor. *J. Biol. Chem.* **279**, 51 804–51 816. (doi:10.1074/jbc.M406581200)
39. Guthrie GJ, Aydemir TB, Troche C, Martin AB, Chang SM, Cousins RJ. 2015 Influence of ZIP14 (slc39A14) on intestinal zinc processing and barrier function. *Am. J. Physiol. Gastrointest. Liver Physiol.* **308**, G171–G178. (doi:10.1152/ajpgi.00021.2014)
40. Haase H, Ober-Blobaum JL, Engelhardt G, Hebel S, Heit A, Heine H, Rink L. 2008 Zinc signals are essential for lipopolysaccharide-induced signal transduction in monocytes. *J. Immunol.* **181**, 6491–6502. (doi:10.4049/jimmunol.181.9.6491)
41. Knoell DL, Julian MW, Bao S, Besecker B, Macre JE, Leikauf GD, DiSilvestro RA, Crouser ED. 2009 Zinc deficiency increases organ damage and mortality in a murine model of polymicrobial sepsis. *Crit. Care Med*. **37**, 1380–1388. (doi:10.1097/CCM.0b013e31819cefe4)
42. Prasad AS. 2008 Zinc in human health: effect of zinc on immune cells. *Mol. Med.* **14**, 353–357. (doi:10.2119/2008-00033.Prasad)
43. Bao S, Knoell DL. 2006 Zinc modulates cytokine-induced lung epithelial cell barrier permeability. *Am. J. Physiol. Lung Cell Mol. Physiol.* **291**, L1132–L1141. (doi:10.1152/ajplung.00207.2006)
44. Liu J *et al*. 2011 Demand for Zn^{2+} in acid-secreting gastric mucosa and its requirement for intracellular Ca^{2+}. *PLoS ONE* **6**, e19638. (doi:10.1371/journal.pone.0019638)